Effects of Concentration of Some Lanthanide(III) Complexes of 1,7-Bis(carboxymethyl)-1,4,7,10-tetraazacyclododecane on Bis(*p*-nitrophenyl)-phosphate Hydrolysis[‡]

C. Allen Chang,*[a] Bo Hong Wu,[a] and Chih-Hsiang Hsiao[a]

A detailed study of the effects of the concentration of some lanthanide(III) complexes [LnDO2A$^+$; DO2A = 1,7-bis(carboxymethyl)-1,4,7,10-tetraazacyclododecane] on the hydrolysis of the phosphodiester bond of the compound BNPP [sodium bis(4-nitrophenyl)phosphate] is reported at 25 °C and pH 7.90 (Ln = Eu), 9.35 (Ln = Eu), and 9.90 (Ln = Eu, Er and Yb). The reaction is found to be first order with respect to BNPP concentration at pH 7.90 and 9.35 and to increase to 1.78 ± 0.09, 1.64 ± 0.07, and 1.63 ± 0.09 with respect to [EuDO2A$^+$] concentration at pH 7.90, 9.35, and 9.90, respectively, thereby indicating that dinuclear species are involved in the reactions. Similar observations were found for the other two LnDO2A$^+$ complexes at pH 9.90 [1.63 ± 0.11 (Er) and 1.49 ± 0.09 (Yb)]. The k_{obs} data obtained by the initial rate method could be fitted to a monomer-dimer reaction model for all LnDO2A$^+$ complexes at pH 7.90, 9.35, and 9.90 in the [LnDO2A$^+$] concentration range 1.0–20.0 mM. The dinuclear species, namely the mono-hydroxo-bridged complexes [Ln$_2$(DO2A)$_2$(µ-OH)(OH)(H$_2$O)$_{n = 1–3}$] and the di-hydroxo-bridged complexes [Ln$_2$(DO2A)$_2$(µ-OH)$_2$(H$_2$O)$_{n = 0–2}$] are found to be more reactive, with reactivities in the order Eu > Yb > Er. The overall formation constants for [Ln$_2$(DO2A)$_2$(µ-OH)$_2$(H$_2$O)$_n$]-BNPP are around 10^4 M^{-1}. The EuDO2A$^+$-promoted BNPP hydrolysis rates are similar to, or up to two orders of magnitude faster than, most of those reported for other lanthanide and transition-metal complexes. (© Wiley-VCH Verlag GmbH & Co. KGaA, 69451 Weinheim, Germany, 2009)

Introduction

We have been interested in the design, synthesis, and characterization of artificial nucleases and ribonucleases containing macrocyclic lanthanide (Ln) complexes because their high thermodynamic stability, low kinetic lability, high coordination number, and charge density (Lewis acidity) allow greater design flexibility, specificity, and stability.[1–5] Due to the complicated hydrolytic properties and potential Ln-hydroxide polynuclear cluster formation of cationic lanthanide complexes, the design of efficient agents and the elucidation of possible mechanisms for the promotion of phosphodiester hydrolysis remains a challenge.

Previously we have reported the effects of pH, metal-ion radius, the number of inner-sphere coordinated water molecules, and the charge and concentration of a number of lanthanide complexes on the promotion of BNPP phosphodiester bond hydrolysis.[1,2] In general, faster BNPP hydrolysis rates were observed for lanthanide complexes with stronger lanthanide ion Lewis acidity, a greater number of inner-sphere coordinated water molecules, and greater positive charge on the complex. However, complex formation sometimes alters the expected trends in that it may cause changes in the pK_h values of inner-sphere-coordinated water molecules and/or may result in active or inactive dimer or higher-order oligomers. This is particularly evident for the heavier lanthanide complexes.[1,2,6]

A preliminary study of the effects of the concentration of the europium(III) complex of 1,7-bis(carboxymethyl)-1,4,7,10-tetraazacyclododecane (EuDO2A$^+$) on the promotion of BNPP hydrolysis has also been conducted.[1] The observed BNPP hydrolysis rate constant vs. [EuDO2A$^+$] concentration at pH 9.35 were fitted to a monomer-dimer reaction model and the dimer rate constant found to be 400 times greater than that of the monomer. However, only five data points were involved in the [EuDO2A$^+$] concentration range 1.0–4.75 mM. In order to understand more about the effects of concentration of the lanthanide complex BNPP hydrolysis, and to elucidate possible mechanisms, we have conducted further studies at three solution pH values (7.90, 9.35, and 9.90) over a wider concentration range (1.0–20.0 mM). For comparison, the reactions between LnDO2A$^+$ (Ln = Er and Yb) and BNPP at pH 9.90 were also studied. This paper reports our findings.

Results and Discussion

Initial Rate Studies

Hydrolysis of BNPP produces 4-nitrophenolate ion, which has an absorption maximum at 400 nm. As some of the reactions proceeded rather slowly, initial rate methods were used to determine the orders of the reactions and the pseudo-first-order rate constants. The observed initial rates were measured by monitoring the absorbance changes at 400 nm with time and the pseudo-first-order rate constants (k_{obs}) were obtained by dividing the initial rate values by $[BNPP]_0$, the initial concentration of BNPP. Note that the calculated first-order BNPP hydrolysis rate constant by NaOH[1] was 2.3×10^{-5} M^{-1} s^{-1}. Controlled BNPP hydrolysis reactions using only the buffer solutions without lanthanide complexes were always studied as references in all studies; the rates were always negligible.

Solution pH values of 7.90 and 9.35 were initially selected for the present studies because the pK_h value of $EuDO2A^+$ is 8.1.[7] At pH 7.90, only 39% of $EuDO2A^+$ hydrolyzes, whereas at pH 9.35 95% of $EuDO2A^+$ is in the hydrolyzed form. Figure 1 shows plots of absorbance vs. time for the $EuDO2A^+$-promoted BNPP hydrolysis reaction at a $EuDO2A^+$ concentration of 1.0 mM and various BNPP concentrations (0.2–8.0 mM). The initial rate data could be obtained from these plots (the data for [BNPP]-dependence studies are listed in Table S1 in the Supporting Information). Theoretically, the rate can be defined as: rate = k $[BNPP]^x[EuDO2A^+]^y$. A plot of the log(initial rates) vs. log[BNPP] would therefore give an intercept value of $log(k[EuDO2A^+]^y)$ and a slope value x, which is the order of the reaction with respect to BNPP concentration. The log plots (not shown) give the respective slope values 0.98 ± 0.03 ($r^2 = 0.999$) and 0.99 ± 0.02 ($r^2 = 0.998$) at pH 7.90 and 9.35, respectively, thereby indicating that the reaction is first order in BNPP concentration.
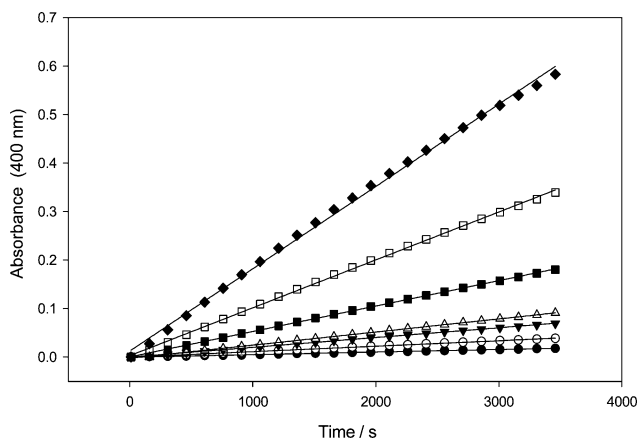
However, similar plots of log(initial rates) vs. $log[EuDO2A^+]$ at a BNPP concentration of 0.10 mM give the respective slope values 1.78 ± 0.09, 1.64 ± 0.07, and 1.63 ± 0.09 at pH 7.90, 9.35, and 9.90 ($[EuDO2A^+]$ = 1.0–20.0 mM), respectively, thereby indicating that the reaction with respect to $[EuDO2A^+]$ is complicated and dinuclear species are involved in the reactions (Figure 2). The reaction rates also increase with increasing pH (see below). To examine whether the orders of the reactions with respect to the concentration of other $LnDO2A^+$ cations showed similar behaviors, we also determined the initial rates of $LnDO2A^+$ (Ln = Er and Yb) reactions with BNPP at pH 9.90. The plots of log(initial rates) vs. $log[LnDO2A^+]$ are also shown in Figure 2 and the slopes of the linear regression analysis gives the reaction orders 1.63 ± 0.11 (Er) and 1.49 ± 0.09 (Yb). Again, the data show that dinuclear species are also involved in the reactions with Er^{III} and Yb^{III}.
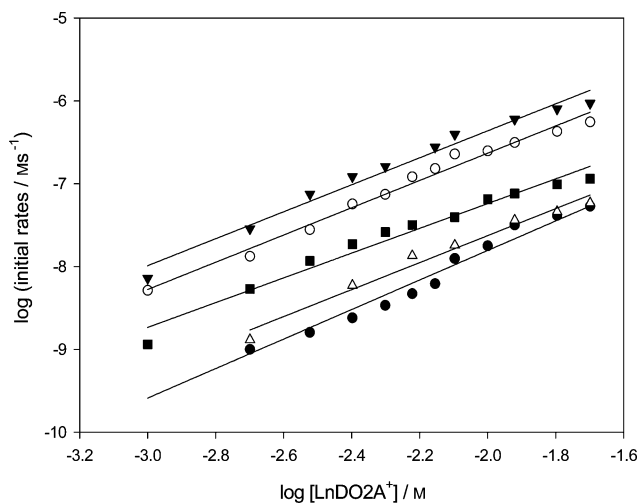

Figure 2. Log(initial rate) plots for the BNPP reactions with $LnDO2A^+$: (●) $EuDO2A^+$, pH 7.90; (○) $EuDO2A^+$, pH 9.35; (▼) $EuDO2A^+$, pH 9.90; (△) $ErDO2A^+$, pH 9.90; (■) $YbDO2A^+$, pH 9.90; 25 °C; [BNPP] = 0.10 mM; $[LnDO2A^+]$ = 1.0–20.0 mM; [buffer] = 20 mM; μ = 0.10 M $(CH_3)_4NCl$. Solid lines are the best fits of the linear least-squares regression analyses. All r^2 values are around 1.00.

Effects of $[LnDO2A^+]$ on BNPP Hydrolysis Rates at pH 7.90, 9.35, and 9.90 − Simple Monomer and Monomer-Dimer Reaction Models.

Figure 3 shows the plots of k_{obs} vs. $EuDO2A^+$ concentration at pH 7.90, 9.35, and 9.90. The data are listed in Table S2 in the Supporting Information together with those obtained for $ErDO2A^+$ and $YbDO2A^+$ at pH 9.90 (inset in Figure 3). Note that the data for similar studies for lighter trivalent $LnDO2A^+$ complexes (Ln = La, Ce, Pr, and Nd) were all difficult to reproduce and precipitate formation was observed in the solutions.

Fitting the k_{obs} values in Figure 3 to $LnDO2A^+$ concentration according to the simple monomer reaction model depicted in Scheme 1 [Equation (1)] gives the second-order rate constants k_1 and third-order rate constants k_2, which

Figure 1. Plots of absorbance at 400 nm vs. time (s) for the $EuDO2A^+$-promoted BNPP hydrolysis reaction. $[EuDO2A^+]$ = 1.0 mM; [BNPP] = 0.2 (●), 0.4 (○), 0.8 (▼), 1.0 (△), 2.0 (■), 4.0 (□), 8.0 mM (◆); 25 °C; pH 7.90; [MPS buffer] = 20 mM; μ = 0.10 M $(CH_3)_4NCl$. Solid lines are the best fits of linear least-squares regression analyses. All r^2 values are around 1.00.
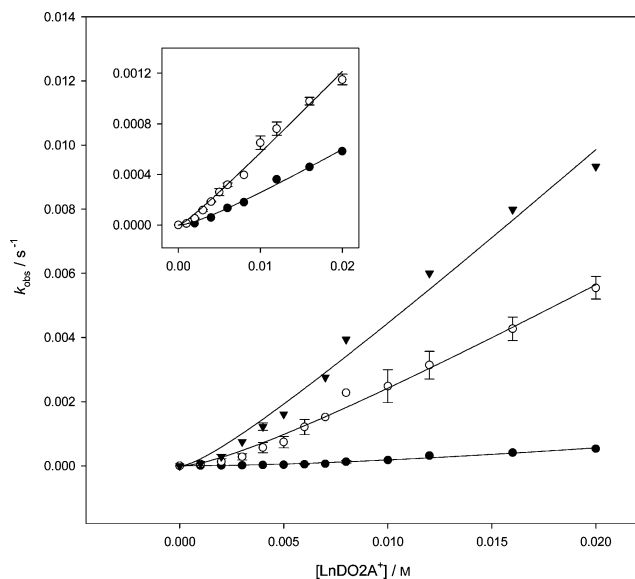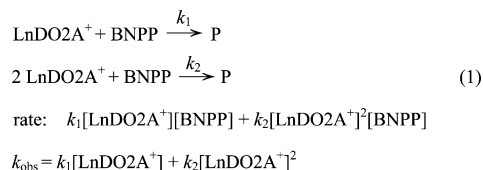
Figure 3. Plots of the pseudo-first-order rate constants of BNPP hydrolysis vs. the concentration of LnDO2A$^+$: EuDO2A$^+$: (●) pH 7.90, (○) pH 9.35, (▼) pH 9.90. Inset: ErDO2A$^+$: (●) pH 9.90 and YbDO2A$^+$ (○) pH 9.90. 25 °C, [BNPP] = 0.10 mM, [buffer] = 20 mM, μ = 0.10 M (CH$_3$)$_4$NCl. The solid lines were calculated based on the best non-linear least-squares fits according to the monomer-dimer reaction model shown in Scheme 2.

are listed in Table 1. However, this model is not desirable because it does not account for the tendency of "rate saturation" at high LnDO2A$^+$ concentration and particularly because it is known that cationic lanthanide complexes can form "hydrate-, hydroxo-, or oxo-bridged" species at high pH (>pH 6.5) due to the presence of inner-sphere coordinated water molecules/hydroxide ions, thereby altering their reactivity.[8] The correlation coefficients (i.e. r^2 values) and standard errors of estimate (SEEs) are also much larger than those of the other fits (see below).

$$\text{LnDO2A}^+ + \text{BNPP} \xrightarrow{k_1} \text{P}$$

$$2\,\text{LnDO2A}^+ + \text{BNPP} \xrightarrow{k_2} \text{P} \qquad (1)$$

rate: $k_1[\text{LnDO2A}^+][\text{BNPP}] + k_2[\text{LnDO2A}^+]^2[\text{BNPP}]$

$k_{\text{obs}} = k_1[\text{LnDO2A}^+] + k_2[\text{LnDO2A}^+]^2$

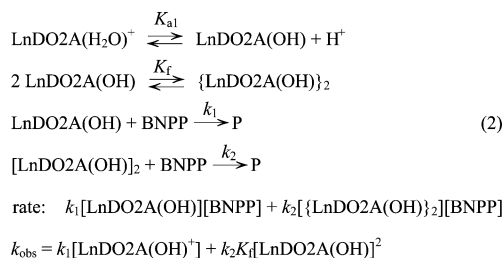Scheme 1. A simple monomer reaction model.

Scheme 2 shows a monomer-dimer reaction model where the species LnDO2A(OH) and {LnDO2A(OH)}$_2$ are assumed to be the reactive ones.

Using the following derivations, we can obtain an equation for [LnDO2A(OH)] [Equation (3)].

Substitution of Equation (3) into the rate law [Equation (2)], using a pK_a value of 8.1 for EuDO2A$^+$ and 9.4 for YbDO2A$^+$, and following the method described in previous reports,[1,9,10] allows us to fit the k_{obs} data to [LnDO2A$^+$]$_T$ and obtain k_1, k_2, and K_f values (Table 2). The pK_a value for ErDO2A$^+$ was estimated to be 9.4 by taking it as an unknown parameter for the fit.

Table 1. The fitted equilibrium and rate constant values (Scheme 1) for the reaction of LnDO2A$^+$ with BNPP at pH 7.90, 9.35, and 9.90.

pH	k_1 [M^{-1} s^{-1}]	k_2 [M^{-2} s^{-1}]	r^2	SEE
	EuDO2A			
7.90	0.0165	7.42	0.980	3.50×10^{-5}
9.35	0.197	5.46	0.991	2.00×10^{-4}
9.90	0.398	5.11	0.990	5.00×10^{-4}
	ErDO2A			
9.90	0.0271	0.820	0.994	2.79×10^{-5}
	YbDO2A			
9.90	0.0719	0.466	0.993	5.23×10^{-5}

$$\text{LnDO2A(H}_2\text{O)}^+ \underset{}{\overset{K_{a1}}{\rightleftharpoons}} \text{LnDO2A(OH)} + \text{H}^+$$

$$2\,\text{LnDO2A(OH)} \underset{}{\overset{K_f}{\rightleftharpoons}} \{\text{LnDO2A(OH)}\}_2$$

$$\text{LnDO2A(OH)} + \text{BNPP} \xrightarrow{k_1} \text{P} \qquad (2)$$

$$[\text{LnDO2A(OH)}]_2 + \text{BNPP} \xrightarrow{k_2} \text{P}$$

rate: $k_1[\text{LnDO2A(OH)}][\text{BNPP}] + k_2[\{\text{LnDO2A(OH)}\}_2][\text{BNPP}]$

$k_{\text{obs}} = k_1[\text{LnDO2A(OH)}^+] + k_2K_f[\text{LnDO2A(OH)}]^2$

Scheme 2. A monomer-dimer reaction model.

$[\text{LnDO2A}^+]_T = [\text{LnDO2A(H}_2\text{O)}^+] + [\text{LnDO2A(OH)}] + 2[\{\text{LnDO2A(OH)}\}_2]$

$K_a = [\text{LnDO2A(OH)}][\text{H}^+]/[\text{LnDO2A(H}_2\text{O)}^+]$

$K_f = [\{\text{LnDO2A(OH)}\}_2] / [\text{LnDO2A(OH)}]^2$

$[\text{LnDO2A}^+]_T = [\text{LnDO2A(OH)}][\text{H}^+]/K_a + [\text{LnDO2A(OH)}] + 2K_f[\text{LnDO2A(OH)}]^2$ (3)

$2K_f[\text{LnDO2A(OH)}]^2 + ([\text{H}^+]/K_a + 1)[\text{LnDO2A(OH)}] - [\text{LnDO2A}^+]_T = 0$

$[\text{LnDO2A(OH)}] = \{-([\text{H}^+]/K_a + 1) + (([\text{H}^+]/K_a + 1)^2 + 8K_f[\text{LnDO2A}^+]_T)^{1/2}\}/4K_f$

Table 2. The fitted equilibrium and rate constant values (Scheme 2) for the reaction of LnDO2A$^+$ with BNPP at pH 7.90, 9.35, and 9.90.
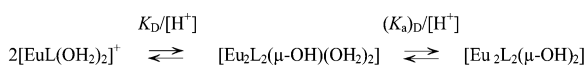
pH	k_1 [M^{-1} s^{-1}]	k_2 [M^{-1} s^{-1}]	K_f [M^{-1}]	r^2	SEE
	EuDO2A				
7.90	4.08×10^{-10}	0.185	104	0.986	2.95×10^{-5}
9.35	3.62×10^{-9}	0.825	191	0.995	2.00×10^{-4}
9.90	3.61×10^{-9}	1.26	409	0.994	4.00×10^{-4}
	ErDO2A				
9.90	4.78×10^{-10}	0.0868	309	0.997	2.23×10^{-5}
	YbDO2A				
9.90	2.27×10^{-9}	0.141	2004	0.994	4.77×10^{-5}

Table 2 clearly shows that the k_1 values are all negligible when compared with their corresponding k_2 values. This is mainly because the dimers are more reactive and their contributions outweigh those of the monomers. If the term $k_1[\text{LnDO2A(OH)}^+]$ is eliminated from Equation (2), the resulting k_2 and K_f values are the same as those obtained

without elimination. The k_2 values increase with increasing pH for EuDO2A$^+$. It should also be noted that the K_f values were obtained using the initial rate data and, because the rate of dimer formation is slow and increases with increasing pH, the value at higher pH is expected to be closer to the real one. The dimer reactivities follow the order {EuDO2A(OH)}$_2$ > {YbDO2A(OH)}$_2$ > {EuDO2A(OH)}$_2$.

More Detailed Monomer-Dimer Reaction Model

Morrow et al. recently reported the transesterification reaction of EuK21DA$^+$ (K21DA = 1,7-diaza-4,10,13-trioxacyclopentadecane-N,N'-diacetate, L) with HpPNP (2-hydroxypropyl-4-nitrophenyl phosphate).[11] An equilibrium model involving dimer formation was proposed for the complex EuK21DA$^+$ (EuL$^+$) at pH above 8 based on the pH titration data.

$$2[\text{EuL(OH}_2)_2]^+ \underset{}{\overset{K_D/[\text{H}^+]}{\rightleftharpoons}} [\text{Eu}_2\text{L}_2(\mu\text{-OH})(\text{OH}_2)_2] \underset{}{\overset{(K_a)_D/[\text{H}^+]}{\rightleftharpoons}} [\text{Eu}_2\text{L}_2(\mu\text{-OH})_2]$$

EuK21DA$^+$ has two inner-sphere coordinated water molecules.[12] In this model, it was proposed that EuK21DA$^+$ could form an active dimer with one bridging μ-OH group, and an inactive dimer with two bridging μ-OH groups. The observed HpPNP transesterification rate constants could be fitted to the equation below where k_{Mon} and k_{Di} are the respective rate constants for the active monomeric and dimeric complexes. It was found that the dimeric species was more reactive.
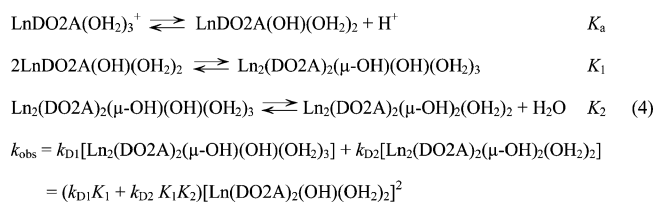
$$k_{\text{obs}} = k_{\text{Mon}}[\text{EuL(OH}_2)_2] + k_{\text{Di}}[\text{Eu}_2\text{L}_2(\mu\text{-OH})(\text{OH}_2)_2]$$

For LnDO2A$^+$ complexes, the complex-formation reactions between Ln^{3+} and DO2A are very slow, thus making it difficult to establish an exact equilibrium model at high pH. However, laser fluorescence studies confirmed that three inner-sphere coordinated molecules are present for EuDO2A$^+$. It was also found that there are at least three species present with emission peaks at 579.33, 580.0 (shoulder), and 580.25 nm.[7] The peaks at 579.33 and 580.25 nm were initially assigned to EuDO2A(OH$_2$)$_3$$^+$ and EuDO2A-(OH)(OH$_2$)$_2$; the shoulder at 580.0 nm was not assigned. It was found previously that 1:1 and 1:2 Eu$^{\text{III}}$-EDTA complexes and similar complexes have spectral maxima close to each other at high pH.[13–15] Thus, it is possible that the

shoulder at 580.0 nm and the peak at 580.25 nm may indicate potentially more complicated equilibria between EuDO2A(OH)(OH$_2$)$_2$ and OH-bridged dimers (see below).

In another paper by Merbach et al.,[16] the absorption spectrum of EuDO2A$^+$ has been reported to contain two peaks, one at 579.0 nm and the other at 579.8 nm, which are in equilibrium at pH 6.4 with an equilibrium constant, K, of 4.0. The former, major peak was assigned to EuDO2A(H$_2$O)$_3$$^+$ and the latter, minor one to EuDO2A-(H$_2$O)$_2$$^+$. If the two species are still in equilibrium at higher pH, the major species EuDO2A(H$_2$O)$_3$$^+$ could form Eu$_2$(DO2A)$_2$(μ-OH)$_2$(OH$_2$)$_2$, which contains two inner-sphere coordinated water molecules and would still be active to catalyze the hydrolysis of BNPP. However, the minor species Eu$_2$(DO2A)$_2$(μ-OH)$_2$, which has no inner-sphere coordinated water molecule, would be inactive to catalyze BNPP hydrolysis.

Scheme 3 shows a more detailed monomer-dimer reaction model which assumes that two dimers, namely the mono-hydroxo-bridged complex [Ln$_2$(DO2A)$_2$(μ-OH)(OH)(OH$_2$)$_2$] and the di-hydroxo-bridged complex [Ln$_2$(DO2A)$_2$(μ-OH)$_2$(OH$_2$)$_2$], are present in equilibrium. If the reactivities of the monomeric LnDO2A(OH$_2$)$_3$$^+$ and LnDO2A-(OH)(OH$_2$)$_2$ species are assumed to be negligible (see above) with respect to the active dimeric species, and by using the equilibrium model shown in Scheme 3, one can obtain values for K_1, K_2, k_{D1}, and k_{D2} by fitting the rate data to Equation (4); the results of this fitting are listed in Table 3. The quantities [LnDO2A(OH)(OH$_2$)$_2$], [Ln$_2$(DO2A)$_2$-(μ-OH)(OH)(OH$_2$)$_3$], and [Ln$_2$(DO2A)$_2$(μ-OH)$_2$(OH$_2$)$_2$] can be calculated by the derivations shown in the Supporting Information using mass balance and corresponding equilibrium expressions.

$$\text{LnDO2A(OH}_2)_3{}^+ \rightleftharpoons \text{LnDO2A(OH)(OH}_2)_2 + \text{H}^+ \qquad K_a$$

$$2\text{LnDO2A(OH)(OH}_2)_2 \rightleftharpoons \text{Ln}_2(\text{DO2A})_2(\mu\text{-OH})(\text{OH})(\text{OH}_2)_3 \qquad K_1$$

$$\text{Ln}_2(\text{DO2A})_2(\mu\text{-OH})(\text{OH})(\text{OH}_2)_3 \rightleftharpoons \text{Ln}_2(\text{DO2A})_2(\mu\text{-OH})_2(\text{OH}_2)_2 + \text{H}_2\text{O} \quad K_2 \quad (4)$$

$$k_{\text{obs}} = k_{\text{D1}}[\text{Ln}_2(\text{DO2A})_2(\mu\text{-OH})(\text{OH})(\text{OH}_2)_3] + k_{\text{D2}}[\text{Ln}_2(\text{DO2A})_2(\mu\text{-OH})_2(\text{OH}_2)_2]$$

$$= (k_{\text{D1}}K_1 + k_{\text{D2}}K_1K_2)[\text{Ln(DO2A})_2(\text{OH})(\text{OH}_2)_2]^2$$

Scheme 3. A more detailed monomer-dimer reaction model.

The product K_1K_2 for each LnDO2A$^+$ complex in Table 2 is equal to the corresponding K_f value in Table 1 in all cases, thus indicating that the more detailed model
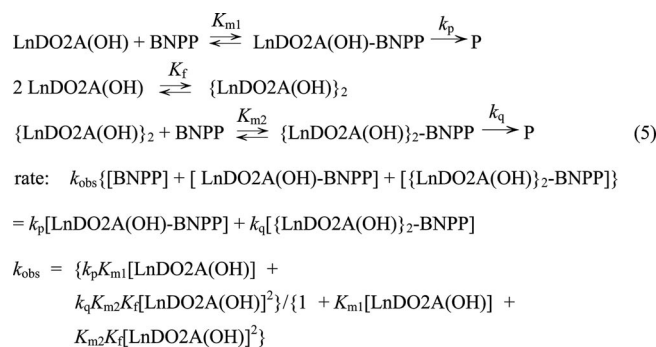
Table 3. The fitted equilibrium and rate constant values (Scheme 3) for the reaction of LnDO2A$^+$ with BNPP at pH 7.90, 9.35, and 9.90.

pH	k_{D1} ($\text{M}^{-1}\text{s}^{-1}$)	k_{D2} ($\text{M}^{-1}\text{s}^{-1}$)	K_1 [M^{-1}]	K_2	r^2	SEE
			EuDO2A			
7.90	1.15	0.122	6.29	15.6	0.986	3.29×10^{-5}
9.35	1.97	0.814	1.97	96.0	0.995	2.00×10^{-4}
9.90	129	0.688	1.85	220	0.994	4.00×10^{-4}
			ErDO2A			
9.90	0.139	0.0866	1.36	226	0.997	2.49×10^{-5}
			YbDO2A			
9.90	6.97	0.131	2.69	744	0.994	5.06×10^{-5}

(Scheme 3) is consistent with that shown in Scheme 2. The correlation coefficients and SEEs are either equal to, or slightly higher than, those of the corresponding values obtained by fitting to the model in Scheme 2. It is interesting to observe that the k_{D1} values are all greater than their corresponding k_{D2} values, which indicates that the reactivity of the mono-hydroxo-bridged complex {$Ln_2(DO2A)_2(\mu$-OH)(OH)(OH$_2$)$_3$} is greater than that of its di-hydroxo-bridged analogue {$Ln_2(DO2A)_2(\mu$-OH)$_2$(OH$_2$)$_2$}. This is expected because a non-bridged, coordinated hydroxide ion should be more reactive than a bridging hydroxide ion. However, the concentration of the mono-hydroxo-bridged dimer is smaller than that of the di-hydroxo-bridged dimer due to its smaller equilibrium constant K_1.

Reaction Models Involving Ln-Dimer-BNPP Formation Equilibrium

The mechanistic models depicted in Schemes 2 and 3 still cannot account for the tendency of rate saturation at higher $[LnDO2A^+]_T$. Thus, the model depicted in Scheme 4 was proposed for data fitting.[17]

$$LnDO2A(OH) + BNPP \xrightleftharpoons{K_{m1}} LnDO2A(OH)\text{-}BNPP \xrightarrow{k_p} P$$

$$2\, LnDO2A(OH) \xrightleftharpoons{K_f} \{LnDO2A(OH)\}_2$$

$$\{LnDO2A(OH)\}_2 + BNPP \xrightleftharpoons{K_{m2}} \{LnDO2A(OH)\}_2\text{-}BNPP \xrightarrow{k_q} P \qquad (5)$$

rate: $k_{obs}\{[BNPP] + [\,LnDO2A(OH)\text{-}BNPP] + [\{LnDO2A(OH)\}_2\text{-}BNPP]\}$

$= k_p[LnDO2A(OH)\text{-}BNPP] + k_q[\{LnDO2A(OH)\}_2\text{-}BNPP]$

$k_{obs} = \{k_p K_{m1}[LnDO2A(OH)] +$
$\quad k_q K_{m2} K_f[LnDO2A(OH)]^2\}/\{1 + K_{m1}[LnDO2A(OH)] +$
$\quad K_{m2}K_f[LnDO2A(OH)]^2\}$

Scheme 4. A monomer-dimer saturation reaction model.

The quantities [BNPP] and [LnDO2A(OH)] can be derived from mass balance and equilibrium expressions, as shown in the Supporting Information. Assuming that the contribution from the term $k_p K_{m1}[LnDO2A(OH)]$ to the overall k_{obs} is negligible (see above), and that $[BNPP]_T = 0.0001$ M, the simplified Equation (6) can be obtained.

$$k_{obs} = \{k_q K_{m2} K_f[LnDO2A(OH)]^2\}/\{1 + K_{m2}K_f[LnDO2A(OH)]^2\} \qquad (6)$$

The quantity [LnDO2A(OH)] can be calculated from Equation (3) using the appropriate pK_a values. The results of fitting the rate data to Equation (6) are listed in Table 4, and Figure 4 shows that rate saturation can indeed be accounted for by the model shown in Scheme 4. This model also allows us to estimate the K_{m2} values from the data in Table 4 [K_{m2} values are in the order of 10^2–10^3 M^{-1} (not considering the pH 7.90 data)]. Note that the K_{m2} and K_f values are subject to larger variations, particularly with respect to pH, which may be caused by the nature of the data and the assumptions made to simplify the data fitting.

However, the logarithmic average of the $K_{m2}K_f$ values, in other words the overall formation constant value for {$LnDO2A(OH)$}$_2$-BNPP, is 3.9 ± 0.2, which suggests that the precision is quite acceptable. The exact nature of the active dimeric ErDO2A and YbDO2A species is unclear. However, if there are only two coordinated water molecules at the lanthanide ion at low pH, the active species at high pH is likely to be {$Ln_2DO2A_2(\mu$-OH)(OH)(OH$_2$)}.

Table 4. The fitted equilibrium and rate constants (Scheme 4) for the reaction of LnDO2A$^+$ with BNPP at pH 7.90, 9.35 and 9.90.

pH	k_q [s^{-1}]	K_{m2} [M^{-1}]	K_f [M^{-1}]	r^2	SEE
		EuDO2A			
7.90[a]	0.00144	2.88×10^4	0.357	0.990	2.53×10^{-5}
9.35	0.0133	208	21.3	0.997	2.00×10^{-4}
9.90	0.0137	4.75×10^3	1.28	0.999	1.00×10^{-4}
		ErDO2A			
9.90	1.10×10^{-3}	648	10.8	0.999	1.40×10^{-5}
		YbDO2A			
9.90	2.24×10^{-3}	271	46.4	0.998	2.91×10^{-5}

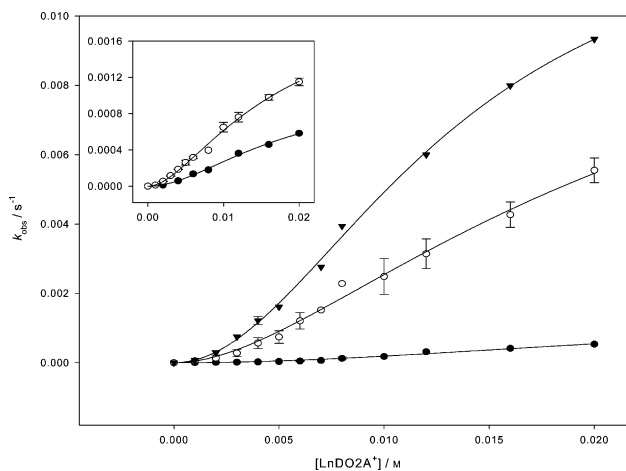[a] The data for pH 7.90 are subject to a relatively large error.

Figure 4. Plots of the pseudo-first-order rate constants of BNPP hydrolysis vs. the concentration of LnDO2A$^+$. EuDO2A$^+$: (●) pH 7.90, (○) pH 9.35, (▼) pH 9.90. Inset: ErDO2A$^+$: (●) pH 9.90 and YbDO2A$^+$: (○) pH 9.90. 25 °C, [BNPP] = 0.10 mM, [buffer] = 20 mM, μ = 0.10 M (CH$_3$)$_4$NCl. The solid lines were calculated based on the best non-linear least-squares fits according to the monomer-dimer saturation reaction model in Scheme 4.

A variation of the model shown in Scheme 4 is available in the Supporting Information (Scheme S1),[17] where data analysis is also discussed. The correlation coefficients for these two models are closer to unity, and the SEEs are smaller than those for the models in Schemes 2 and 3. Thus, models 4 and S1 are mathematically better than models 2 and 3. More detailed comparisons of the mechanistic models in Schemes 2, 3, 4, and S1 are also provided in the Supporting Information.

Time-Dependent Laser-Excited Fluorescence and ESI-MS Studies

The laser-excited fluorescence spectra of EuDO2A$^+$ solutions (0.1 mM) were measured at pH 8, 9, and 10 at 0, 6, and 24 h after sample preparation (Figure S1 in the Supporting Information). It can be seen that the three peaks (species) at 579.33, 580.0, and 580.25 nm reach equilibrium within 6 h. Between 6 and 24 h, the intensities of the peak at 580.25 nm and the shoulder at 580.0 nm remain roughly unchanged for all solution pH's. In separate experiments, the reactivity of EuDO2A$^+$-promoted BNPP hydrolysis was found to decrease with increasing "standing" time after EuDO2A$^+$ solution preparation, particularly at high pH.[18] This implies that although the peak intensities at 580.25 and 580.0 nm do not change very much, the species involved must have been converted into less reactive ones with similar fluorescence spectral properties.

We have also performed ESI-MS measurements to examine whether EuDO2A$^+$ dimer formation is present in the reaction mixture. The preliminary results show that although some m/z data could be used as evidence, there is still the possibility of gas-phase dimerization which could make this evidence a "false-positive".[18] Previous potentiometric titration data, on the other hand, did not confirm the presence of dimer formation.[7,19] This is mainly due to the fact that the entire complexation process between trivalent lanthanide ions and DO2A is very slow, which makes the determination of stability constants for monomeric lanthanide complexes, not to mention hydroxo-dimer formation, very difficult. Indeed, two sets of LnDO2A$^+$ complex stability constants have been reported.[7,20] Unless this issue is resolved, complete and reliable speciation studies will be difficult, and attempts to use such information to propose potential reactive species would be futile. Nevertheless, it is highly possible that very reactive dimers are formed during the initial reaction stages but in very small amounts. Efforts to obtain single crystals for structural determination as additional support for the above explanations were unsuccessful, probably because more than one heterogeneous hydroxide species is formed in solution.

Comparisons of LnDO2A-BNPP Reaction Models and Rates with Other Lanthanide and Transition Metal Complex Systems

In some cases, and at three different solution pH's (7.90, 9.35, 9.90) and with two sets of different reaction models (i.e. Schemes 2/3 and Schemes 4/S1), the dimer formation equilibrium constant K_f values for trivalent lanthanide-DO2A complexes were fitted to be in the ranges 138–2003 M^{-1} (Schemes 2 and 3) and 0.4–46 M^{-1} (Scheme 4). In a more relevant study, Yatsimirsky, et al. have reported on the lanthanide-BTP [bis(tris-propane)] system,[19] whose potentiometrically determined logarithmic overall dimer formation constant in the form of [2BTP-2Eu-2OH]/[Eu]^2-[BTP]^2[OH]^2, in other words log([2BTP-2Eu-2OH]/[Eu]^2-[BTP]^2[OH]^2), is 23.62. To compare the two values, it is nec-

essary to convert the dimer formation expression to be of the same form. Assuming [BTP-Eu]/[BTP][Eu] = 10$^{2.44}$ (that of the Eu^{III}-tris formation constant[21]), [BTP-Eu-OH][H$^+$]/[BTP-Eu] = 10$^{-8.38}$ (that of the hydrolysis constant of Eu^{III}), and [H$^+$][OH$^-$] = 10$^{-13.8}$, and substituting these values into the original equation, gives [BTP-2Eu-2OH]/[BTP-Eu-OH]^2 = 10$^{7.90}$. This value is at least five to six orders of magnitude greater than that of {EuDO2A(μ-OH)}$_2$ dimer formation. This discrepancy could be attributed to a possible over-estimation of the BTP-Eu-OH dimer formation constant and an under-estimation of that of the {EuDO2A(μ-OH)}$_2$ dimer. Note that our data were obtained using the initial rate data, which tend to be lower than the actual values. If the BTP-Eu formation constant is assumed to be similar to that of La-bis-Tris[22] (10$^{4.70}$), then [BTP-2Eu-2OH]/[BTP-Eu-OH]^2 would be 10$^{2.82}$, which is of a similar order of magnitude to that determined using the Scheme 2/3 kinetic approach.

A comparison of the Scheme 2/3 fitting data (at pH 7.90, 9.35, and 9.90) with those reported by others for the transition metal and lanthanide complexes-BNPP hydrolysis systems,[6,9,10,18,23–31] it becomes clear that the k_2, k_{D1}, and k_{D2} values for our lanthanide dimeric complexes are in the range 0.1–129 M^{-1} s^{-1}, which are similar to, or at least two orders of magnitude greater than, those of transition metal complexes reported by others (k_2 values of 10^{-4}–10^{-1} M^{-1} s^{-1}).

The binding constants of Cu^{II} complexes with BNPP and structural analogues are similar to those of the lanthanide complexes. For example, the Cu^{II}-N3 macrocyclic complex–ethyl 4-nitrophenyl phosphate binding constant[9] is around 15 M^{-1}, and the respective ethyl 4-nitrophenyl phosphate and BNPP binding constants are around 20 and 10^2 M^{-1}, respectively, for the mononuclear Cu^{II}-bipyridine complex derivatives.[23,31] On the other hand, the respective LnDO2A(OH)-BNPP and {LnDO2A(μ-OH)}$_2$-BNPP overall formation constants are of the order of 10^0–10^2 and 10^3–10^4 M^{-1}, in other words similar to those found for LnHEDTA(OH)–BNPP (2–147 M^{-1})^2 and Ln^{3+}-BNPP (ca. 10^3 M^{-1}).[6] Although the formation of {LnDO2A(μ-OH)}$_2$ at higher pH results in zero net charge, which diminishes the extent of binding with the negatively charged BNPP, the dinuclear nature of the complex compensates somewhat for the loss of binding strength. Note that strong substrate binding may prevent loss of the reacted substrates and poison the catalyst. The half-lives of cobalt(III) complex systems for BNPP hydrolysis have been reported to be less than a couple of hundred seconds,[25] whereas the binding with BNPP was too strong to be used repeatedly.

The system studied by Martell et al., where a dinuclear La-macrocyclic complex is used in a 3:1 ratio to hydrolyze BNPP, is worth mentioning.[29] At pH 8, the fourth-order rate constant for this system was calculated to be k = 4 × 10^8 M^{-3} s^{-1}. Such a fast rate is attributed to a simultaneous six-metal nuclear reaction. The rate constants calculated for our best case, in other words {EuDO2A(μ-OH)}$_2$ at pH 9.9 (second-order rate constants for the reactions in Schemes 2/3 of around 10^{-1}–10^2 M^{-1} s^{-1}) are lower than

those reported by Martell but similar to, or greater than, those reported by Yatsimirsky (second-order rate constants of around 0.1–1.0 $M^{-1}s^{-1}$).[18,30]

Conclusions

Trivalent lanthanide ions are good Lewis acids for the promotion of BNPP hydrolysis, although they need ligands to form complexes in order to prevent uncontrolled lanthanide hydroxide or oxide formation (ligand-controlled hydrolysis). The properties of the resulting complexes, including charge, steric constraints, the number of inner-sphere coordinated water molecules, etc., are modified by the ligands. We have shown herein that dimeric species such as the mono-hydroxo-bridged species $\{Ln_2L_2(\mu\text{-OH})(OH)(OH_2)_3\}$ and the di-hydroxo-bridged species $\{Ln_2L_2(\mu\text{-OH})_2(OH_2)_2\}$ are potentially more reactive for promoting BNPP hydrolysis. These discoveries could be applicable to the design of better and more stable macrocyclic lanthanide complex reagents for phosphodiester bond hydrolysis, and studies along these lines are currently underway.

Experimental Section

Sample Preparation: Materials and standard solutions were obtained and standardized according to previously reported procedures.[1] Analytical reagent-grade chemicals and buffers, unless otherwise stated, were purchased from Sigma (St. Louis, MO, USA), Aldrich (Milwaukee, Wl, USA), or Merck (Darmstadt, Germany) and were used as received without further purification. Disodium ethylenediaminetetraacetic acid (EDTA) was purchased from Fisher. The ligand DO2A·2HCl·H$_2$O was prepared and purified according to a minor modification of a published method.[6] C$_{12}$H$_{24}$N$_4$O$_4$·2HCl·H$_2$O: calcd. C 38.00, H 7.44, N 14.77; found C 37.98, H 7.24, N 14.71. Carbonate-free deionized water was used for all solution preparations. Lanthanide(III) nitrate solutions were standardized by EDTA complexometric titrations using xylenol orange as the indicator. The DO2A ligand solution was standardized by pH titrations and complexometric titrations with standardized calcium chloride solution.[1]

Kinetic Measurements: All lanthanide complex solutions were freshly prepared by mixing the metal salt and ligand in a 1.00:1.02 molar ratio. The pH of each solution was adjusted to 6.0–6.5 by adding the appropriate amount of (CH$_3$)$_4$NOH solution. The BNPP solution was then added to each solution and the final pH adjusted by adding an appropriate amount of buffer stock solution and used within 20 min after preparation. MPS [3-(N-morpholino)-propanesulfonic acid], TAPS (3-{[tris(hydroxymethyl)methyl]-amino}propanesulfonic acid), CHES [2-(cyclohexylamino)ethanesulfonic acid], and CAPS [3-(cyclohexylamino)-1-propanesulfonic acid], with the respective pK_a values 7.2, 8.4, 9.3, and 10.4, were used to prepare buffer solutions with the desired pH. The initial rates of the lanthanide-complex-promoted BNPP hydrolysis reactions were determined by monitoring spectrophotometrically the absorbance (400 nm) change with time due to the production of 4-nitrophenolate ion from BNPP. The absorbance at 400 nm due to 4-nitrophenol (i.e. less than 0.2% in all cases) was corrected for all solutions. Corrections for the spontaneous hydrolysis of the BNPP substrate in the buffer solutions were not necessary as they were negligible.[1] The concentration of 4-nitrophenolate ion produced

was calculated from the extinction coefficient (18,700 $M^{-1}cm^{-1}$, 400 nm). The initial rate of each reaction was obtained directly from the slope of the plot of 4-nitrophenolate ion concentration vs. time (i.e. up to 500 s for pH 7.90 data and 250 s for pH 9.35 and 9.90 data to ensure less than 5% of the reaction). All plots were linear with $r^2 \geq 0.98$. All experiments were run at least in duplicate and the reported data represent the average values. Agreement between the calculated initial rates for replicate experiments was within 6% for [BNPP]-dependence studies. The data variations were much greater for the [LnDO2A$^+$]-dependence studies at pH 7.90, 9.35, and 9.90 ($\leq$30%; see Results and Discussion).

For the lanthanide complex concentration-dependence studies, the final BNPP concentration was kept at 0.10 mM and the lanthanide complex concentrations were varied in the range 1.0–20.0 mM to fulfill pseudo-first-order reaction conditions. The ionic strength was adjusted to 0.10 M with (CH$_3$)$_4$NCl. An HP 8453 UV/Vis spectrophotometer was used to measure the absorption increase with time at 400 nm due to the formation of 4-nitrophenolate ion after BNPP hydrolysis.[1] Initial rate constants were calculated from the initial rate data divided by [BNPP]$_0$, the initial concentration of BNPP (1.0×10^{-4} M). Microsoft Excel was used for data treatment and Sigma plot was use for curve fitting.

Laser-excited fluorescence[7] and ESI-MS[2] experiments were performed at the Department of Applied Chemistry, National Chiao Tung University, with instruments similar to those described in published procedures.

[1] C. A. Chang, B. H. Wu, B. Y. Kuan, *Inorg. Chem.* **2005**, *44*, 6646–6654.

[2] C. A. Chang, Y.-P. Chen, C.-H. Hsiao, *Eur. J. Inorg. Chem.* **2009**, in press.

[3] a) B. N. Trawick, A. T. Daniher, J. K. Bashkin, *Chem. Rev.* **1998**, *98*, 939–960; b) M. Oivanen, S. Kuusela, H. Lönnberg, *Chem. Rev.* **1998**, *98*, 961–990; c) N. H. Williams, B. Takasaki, M. Well, J. Chin, *Acc. Chem. Res.* **1999**, *32*, 485–493.

[4] a) *Acid-Promoted Peptide Bond Hydrolysis*, in *Metal Ions in Biological Systems* (Eds.: A. Sigel, H. Sigel), Marcel Dekker Inc., New York, **2003**, vol. 40, chapter 10; b) H.-J. Schneider, A. K. Yatsimirski, *Lanthanide-Catalyzed Hydrolysis of Phosphate Esters and Nucleic Acids*, in *Metal Ions in Biological Systems* (Eds.: A. Sigel, H. Sigel), Marcel Dekker Inc., New York, **2003**, vol. 40, chapter 11; c) M. Komiyama, "*Sequence-Selective Scission of DNA and RNA by Lanthanide Ions and Their Complexes*, in *Metal Ions in Biological Systems* (Eds.: A. Sigel, H. Sigel), Marcel Dekker Inc., New York, **2003**, vol. 40, chapter 12; d) M. Komiyama, *Cutting DNA and RNA*, in *Handbook on the Physics and Chemistry of Rare Earths*, Elsevier, Amsterdam, **2004**, vol. 34, chapter 222.

[5] a) K. New, C. M. Andolina, J. R. Morrow, *J. Am. Chem. Soc.* **2008**, *130*, 14861–14871; b) I. Sanchez-Lombardo, A. K. Yatsimirsky, *Inorg. Chem.* **2008**, *47*, 2514–2525.

[6] A. Roigk, R. Hettich, H.-J. Schneider, *Inorg. Chem.* **1998**, *37*, 751–756.

[7] C. A. Chang, F.-K. Shieh, Y.-L. Liu, Y.-H. Chen, H.-Y. Chen, C.-Y. Chen, *J. Chem. Soc., Dalton Trans.* **1998**, 3243–3248.

C. A. Chang, B. H. Wu, C.-H. Hsiao

[8] P. Hurst, B. K. Takasaki, J. Chin, *J. Am. Chem. Soc.* **1996**, *118*, 9982–9983.

[9] A. K. Deal, J. N. Burstyn, *Inorg. Chem.* **1996**, *35*, 2792–2798.

[10] E. L. Hegg, H. S. Mortimore, C. L. Cheung, J. E. Huyett, D. L. Powell, J. N. Burstyn, *Inorg. Chem.* **1999**, *38*, 2961–2968.

[11] E. R. Farquhar, J. P. Richard, J. R. Morrow, *Inorg. Chem.* **2007**, *46*, 7169–7177.

[12] R. C. Hole, S. L. Klakamp, C. A. Chang, W. D. Horrocks Jr., *Inorg. Chem.* **1990**, *29*, 2651–2658.

[13] M. Latva, J. Kankare, K. Haapakka, *J. Coord. Chem.* **1996**, *38*, 85–99.

[14] A. R. Felmy, Z. Wang, D. A. Dixon, A. G. Joly, J. R. Rustad, M. J. Mason, in *Nuclear Site Remediation: First Accomplishments of the Environmental Management Science Program* (Ed.: P. G. Eller), *ACS Symposium Series*, No. 778, Washington D.C, **2001**, 63–82.

[15] J. N. Mathur, P. Thakur, C. J. Dodge, A. J. Fran*cis*, G. R. Choppin, *Inorg. Chem.* **2006**, *45*, 8026–8035.

[16] F. Yerly, F. A. Dunand, E. Toth, A. Figueirinha, Z. Kovacs, A. D. Sherry, C. F. G. Geraldes, A. E. Merbach, *Eur. J. Inorg. Chem.* **2000**, 1001–1006.

[17] a) K. P. McCue, J. R. Morrow, *Inorg. Chem.* **2001**, *40*, 3786–3796; b) J. Rawlings, A. C. Hengge, W. W. Cleland, *J. Am. Chem. Soc.* **1997**, *119*, 61–65; c) J. Rawlings, W. W. Cleland, A. C. Hengge, *J. Inorg. Biochem.* **2003**, *93*, 61–65.

[18] B. H. Wu, C. A. Chang, unpublished results.

[19] P. Gómez-Tagle, A. K. Yatsimirsky, *Inorg. Chem.* **2001**, *40*, 3786–3796.

[20] J. Huskens, D. A. Torres, Z. Kovacs, J. P. Andre, C. F. G. C. Geraldes, A. D. Sherry, *Inorg. Chem.* **1997**, *36*, 1495.

[21] J.-M. Pfefferie, J.-C. G. Bunzli, *Helv. Chim. Acta* **1989**, *72*, 1487–1494.

[22] S. J. Oh, Y.-S. Choi, S. Hwangbo, S. Bae, J. K. Ku, J. W. Park, *Chem. Commun.* **1998**, 2189–2190.

[23] E. Kovari, R. Kramer, *J. Am. Chem. Soc.* **1996**, *118*, 12704–12709.

[24] K. D. Deal, G. Park, J. Shao, N. D. Chasteen, M. W. Brechbiel, R. P. Planalp, *Inorg. Chem.* **2001**, *40*, 4176–4182.

[25] R. Hettich, H. J. Schneider, *J. Am. Chem. Soc.* **1997**, *119*, 5638–5647.

[26] T. Gajda, Y. Düpre, I. Török, J. Harmer, A. Schweiger, J. Sander, D. Kuppert, K. Hegetschweiler, *Inorg. Chem.* **2001**, *40*, 4918–4927.

[27] A. Roigk, O. V. Yescheulova, Y. V. Fedorov, O. A. Fedorova, S. P. Gromov, H. J. Schneider, *Org. Lett.* **1999**, *1*, 833–835.

[28] P. Karsten, A. Neves, A. J. Bortoluzzi, M. Lanznaster, V. Drago, *Inorg. Chem.* **2002**, *41*, 4624–4626.

[29] P. E. Jurek, A. M. Jurek, A. E. Martell, *Inorg. Chem.* **2000**, *39*, 1016–1020.

[30] F. Aguilar-Perez, P. Gómez-Tagle, E. Collado-Fregoso, A. K. Yatsimirsky, *Inorg. Chem.* **2006**, *45*, 9502–9517.

[31] J. R. Morrow, W. C. Trogler, *Inorg. Chem.* **1988**, *27*, 3387–3394.